Published in final edited form as:
Neuroscience. 2004 ; 127(1): 113–123. doi:10.1016/j.neuroscience.2004.03.062.

PATHOGENESIS OF HIPPOCAMPAL NEURONAL DEATH AFTER HYPOXIA–ISCHEMIA CHANGES DURING BRAIN DEVELOPMENT

C. L. Liu, **B. K. Siesjö**, and **B. R. Hu***
Department of Neurology, University of Miami School of Medicine, PO Box 16960, Miami, FL 33136, USA

Abstract

Transient hypoxia–ischemia (HI) leads to delayed neuronal death in both mature and immature neurons but the underlying mechanisms are not fully understood. To understand whether the pathogenesis of HI-induced neuronal death is different between mature and immature neurons, we used a rat HI model at postnatal days 7 (P7), 15 (P15), 26 (P26) and 60 (P60) in order to investigate ultrastructural changes and active caspase-3 distribution in HI-injured neurons as a function of developmental age. In P7 pups, despite more than 95% of HI-injured neurons highly expressing active caspase-3, most of these active caspase-3-positive neurons revealed mixed features of apoptosis and necrosis (a chimera type) under electron microscopy (EM). Classical apoptosis was observed only in small populations of HI-injured P7 neurons. Furthermore, in rats older than P7, most HI-injured neurons displayed features of necrotic cell death under EM and, concomitantly, active caspase-3-positive neurons after HI declined dramatically. Classical apoptosis after HI was rarely found in neurons older than P15. In P60 rats, virtually all HI-injured neurons showed the shrinkage necrotic morphology under EM and were negative for active caspase-3. These results strongly suggest that pathogenesis of HI-induced neuronal death is shifting from apoptosis to necrosis during brain development.

Keywords

neonatal brain; hypoxia–ischemia; neuronal death; brain maturation; RNase protection assay; electron microscopy

Apoptotic neuronal death takes place during brain development under genetic control. Nuclear chromatin condensation or clumping characterized by electron microscopy (EM) is a hallmark of apoptosis and is remarkably conserved among cell types (Kerr et al., 1972; Wyllie, 1997). It is well documented that pathological conditions including brain hypoxia–ischemia (HI) are able to initiate apoptotic machinery to facilitate cell death through activation of caspase-3 (Blomgren et al., 2003; Olney, 2003). In comparison with apoptosis, necrotic cell death occurs always under pathological conditions. Two types of neuronal injury-induced necrotic morphologies characterized by EM have been described in the literature: one is the conventional cellular lysis with cell swelling followed by rupture to release cell contents; the second type of necrosis is characterized by dilation of subcellular organelles followed by shrinkage of the entire cell. Neuronal cell lysis takes place in the infarct core area after focal brain ischemia (Dodson et al., 1974), while the shrinkage type of necrosis occurs in a delayed manner in vulnerable brain regions after transient brain ischemia, in the penumbral regions after focal ischemia, as well as in regions of excitotoxic

*Corresponding author. Tel: +1-305-243-4854; fax: +1-305-243-7183. bhu@med.miami.edu. .

neuronal death (Siesjö, 1985; Deshpande et al., 1992; Fukuda et al., 1999; Colbourne et al., 1999; Hu et al., 2000b; Olney, 2003). In some cases, mixed features of apoptosis and necrosis can be seen in the same neurons after brain injury (Martin et al., 1998;Ishimaru et al., 1999). The neurons dying during development also adopt one of at least three different morphological types: “apoptotic,” “autophagic,” and “non-lysosomal vesiculate,” which probably reflect the various mechanisms underlying both nuclear and cytoplasmic destruction during cell death in developing neurons (Clarke, 1990).

Biochemical and morphological features of both neuronal apoptosis and necrosis have been repeatedly observed in neonatal HI models (Mehmet et al., 1994; Portera-Cailliau et al., 1997; Martin et al., 1998; Renolleau et al., 1998; Pulera et al., 1998; Ishimaru et al., 1999; Hu et al., 2000a; Nakajima et al., 2000; Sheldon et al., 2001). However, classical apoptotic morphology characterized by EM has never been found in adult neurons after hypoxia or ischemia (Deshpande et al., 1992; Fukuda et al., 1999; Colbourne et al., 1999; Gill et al., 2002). Because each of these types of cell death may involve different molecular and biochemical events, understanding the nature of cell death after HI is important in order to determine effective therapeutic targets. To understand the pathogenesis of HI-induced neuronal death at different stages of brain development, we investigated caspase-3 activation and morphological features of cell death after HI in rats at different developmental ages. We found that caspase-3 was highly enriched in neonatal developing neurons, but decreased dramatically with brain development. Despite striking induction of active caspase-3 in HI-injured neonatal neurons, most of these neurons revealed necrotic features under the electron microscope. Classical apoptosis was observed only in small populations of HI-injured neonatal neurons. Furthermore, classical apoptosis after HI was rarely found in neurons older than postnatal day 15.

EXPERIMENTAL PROCEDURES

HI animal model

Pregnant Wistar rats were purchased from Charles River Laboratories (Wilmington, MA, USA) and housed in individual cages. The newborn rats were housed with their dams until weaning at P21.

All procedures for the animal studies were approved by the Animal Care and Use Committee of the University of Miami (Miami, FL). All the experimental protocols were performed in compliance with the National Institutes of Health guidelines for the care and use of animals. The number of animals used and their suffering were minimized. Brain HI was produced by a combination of ligation of the left common carotid artery (CCA) and systemic hypoxia (8% O_2). Briefly, rats at P7, P15, P26 and P60 were anesthetized with halothane (3.5% induction, 1% maintenance). A midline neck incision was made; thereafter, the left CCA was exposed and ligated permanently. The incision was sutured and the rats were returned to their dams or original cages. Following 1 h of recovery, the rats were placed in a hypoxic chamber through which humidified 8% oxygen with the balance nitrogen flowed for 60 min in groups of P7 and P15 pups, and for 30 min in groups of P26 and P60 rats. The concentration of oxygen flowing through the system was monitored with an Ohmeda 5120 Oxygen Monitor (Madison, WI, USA) during the experiments. The hypoxic duration in different groups of rats was chosen based on our previous experiments (Hu et al., 2000a) and the literature, which showed that these periods produced a similar severity of brain damage in different age groups (Blumenfeld et al., 1992; Towfighi et al., 1997; Towfighi and Mauger, 1998). A hypoxic chamber of 500 ml was used for the P7 and P15 pups, one of 1000 ml for P26, and one of 2000 ml for P60 rats. The hypoxic chambers were partially submerged in a 37 °C water bath to maintain normothermia of the pups or rats during the HI periods. After the periods of HI, the rats were kept in the open chamber for

about 30 min until they showed signs of recovery. The rats were then returned to their dams or cages. The contralateral (non-ischemic) sides of the brains after HI were used as controls. In some cases, rats subjected to carotid ligation without subsequent hypoxia were also used as controls. There was no difference between either of these two controls or between the control of carotid artery ligation and untreated rats in this study. This result is consistent with previous studies showing that rats subjected to either carotid ligation without subsequent hypoxia or hypoxia without the ligation do not exhibit brain damage relative to untreated rats (Blumenfeld et al., 1992; Towfighi et al., 1997; Towfighi and Mauger, 1998). The brains were collected at 6, 24 and 48 h after HI. The tissue samples for biochemical analyses were obtained by freezing the brain *in situ* with liquid nitrogen (Hu et al., 2000a). The rats were perfused with ice-cold 4% phosphate-buffered paraformaldehyde for confocal microscopy, and perfused with 2% paraformaldehyde/2.5% glutaraldehyde in 0.1 M cacodylate buffer for EM. The brains were sectioned with a vibratome at a thickness of 50 μm for confocal microscopy or 120 μm for EM.

EM

Tissue sections from P7, P15, P26 and P60 rats subjected to HI were stained by the conventional osmium–uranium–lead method for transmission EM as described previously (Hu et al., 2000b). Briefly, coronal brain sections were cut at a thickness of 120 μm with a vibratome through the level of the dorsal hippocampus and striatum, then postfixed for 1 h with 4% glutaraldehyde in 0.1 M cacodylate buffer (pH 7.4). Sections were postfixed for 2 h in 1% osmium tetroxide in 0.1 M cacodylate buffer, rinsed in distilled water and stained with 1% aqueous uranyl acetate overnight. The tissue sections were then dehydrated in an ascending series of ethanol to 100% followed by dry acetone, and embedded in Durcopan ACM. Thin sections (0.1 μm) were cut and examined with an electron microscope.

Confocal microscopy and histology

Double-label fluorescence confocal microscopy was performed on 50 μm coronal brain sections (Hu et al., 2000a). The brain sections were from sham-operated control rats and rats subjected to HI followed by 6, 24 and 48 h of recovery for all age groups. A specific antibody against active caspase-3 was obtained from Cell Signaling Technology (Beverly, MA, USA). Brain sections were washed with phosphate-buffered saline (PBS) containing 0.1% Triton X-100 (TX100) for 30 min. Non-specific binding sites were blocked in 3% BSA in PBS/0.1% TX100 for 30 min. The first primary antibodies were diluted 1:250 in PBS/0.1% TX100 and 1% BSA. After incubation overnight at 4 °C, the sections were washed in PBS containing 0.1% TX100, three times 10 min at room temperature. The sections were then incubated for 1 h at room temperature with the fluorescent secondary antibodies, fluorescein-labeled anti-rabbit and lissamine rhodamine-labeled anti-mouse diluted 1:200, or propidium iodide (PI) (15 μg/ml) in PBS containing 1% BSA. Sections were washed several times in PBS/0.1% TX100 and mounted on glass slides (Hu et al., 2000a). The slides were analyzed on a BioRad 1024 laserscanning confocal microscope.

Cell counting was carried out to determine the time course of cell death and the numbers of active caspase-3 positive/negative neurons among total dead cells in each brain region after HI. Counting was conducted in the CA1 pyramidal neuronal layer, and in the upper blade of the dentate gyrus (DG) granule cell layer on confocal microscopic images (see Fig. 1) obtained from five microscopic fields (175 μm×175 μm) with a 60× (oil N.A.) objective on the BioRad 1024 confocal microscope. The average number obtained from the five separate fields in each brain region for each animal was used in the data analysis. The data were obtained from four animals in each group (n=4). The data were expressed as mean±S.D. in absolute numbers of active caspase-3 positive/ negative neurons, or as a percentage of active caspase-3 positive/ negative neurons per total of damaged neurons in a single 60× objective

confocal microscopic field. Two-way analysis of variance was used to assess the effects of age and recovery time on active caspase-3 induction and neuronal death.

Neuronal damage after HI was also evaluated on brain sections stained with a histological method. Paraffin-embedded sections were cut at a thickness of 5 μm, mounted on glass slides, dried and stained with acid fuchsin and thionine. Most damaged neurons stained with fuchsin were shrunken and acidophilic (Auer et al., 1984).

RESULTS

Caspase-3 activation after HI

Brain sections were obtained from rats at different postnatal ages subjected to HI followed by various periods of recovery. They were double-labeled with PI and an antibody specifically against active caspase-3, and they were examined by confocal microscopy. Delayed neuronal death occurred in HI-affected brain regions at about 24–48 h in all age groups (Fig. 1), consistent with previous reports (Blumenfeld et al., 1992; Towfighi et al., 1997; Towfighi and Mauger, 1998; Hu et al., 2000a). In Fig. 1, the red color represents PI staining, and green indicates active caspase-3 (Cas3). PI is a fluorescent dye that stains nucleic acids and is often utilized to stain necrotic cells in culture because it is unable to pass lipid membranes. However, in fixed brain sections, PI is able to penetrate into both normal and damaged cells to stain nucleic acids (Fig. 1). In comparison with the contralateral hemisphere, the injured brain region exhibited diminished PI staining (Fig. 1A, arrows and Fig. 1B, arrowheads), confined to the ipsilateral cortical and hippocampal regions (Fig. 1A and 1B, arrows). PI staining can distinguish normal from damaged neurons by their nuclear size and shape under confocal microscopy. PI-stained neuronal nuclei were normaland sphere-shaped in the contralateral regions, but were shrunken and contained small multi-DNA masses in most HI-injured P7 CA1 neurons and in a portion of HI-injured DG neurons (Fig. 1C, P7, large arrows). PI also revealed a population of round nuclear spherical structures in the HI-injured P7 DG region that were clearly distinguishable from nuclei with small multi-DNA masses (Fig. 1C, P7-DG, small arrows). These densely stained nuclear spheres likely correspond to large DNA balls in apoptotic nuclei identified previously by EM (see below). With increasing age, nuclei gradually became irregular-shaped in the HI-injured CA1 and DG regions (Fig. 1C, red, arrowheads). Neurons exhibiting either multi-DNA masses, or relative large nuclear balls, or irregular-shaped nuclei were dead according to their cellular features observed by EM (see below).

Activation of caspase-3 occurs during normal development and is a key biochemical event for developmental apoptotic cell death. Active caspase-3 positive neurons can only be occasionally found on brain sections from P7 sham-operated control and in the contralateral hemisphere of HI-injured P7 pups, but was dramatically induced in almost all HI-injured neurons of the neocortex, hippocampus and reticular thalamic nucleus of P7 pups (Fig. 1A, P7, green). In comparison with P7 pups (Fig. 1B and 1C, P7, Cas3, green), active caspase-3 markedly declined in P15 rats (Fig. 1B and 1C, P15, Cas3, green). By P26, a small portion of HI-injured neurons with active caspase-3 was still present in the DG area, but virtually absent in the CA1 region (Fig. 1B and 1C, P26, green). HI-injured neurons with active caspase-3 were virtually absent in all HI-damaged brain regions of P60 rats (Fig. 1A–1C). Occasionally, a few positive cells with active caspase-3 (less than 1%) after HI could be found in the inner layer of the ipsilateral DG (Table 1) and striatum near the third ventricle in P60 rats (data not shown). According to their distribution, these caspase-3 positive cells in adult rats after HI were probably progenitor cell-derived immature neurons (Bayer and Altman, 1995).

Ultrastractures of HI-injured neurons at different developmental age

The morphology of HI-injured neurons at different ages was further studied by EM (Figs. 2–6). Figs. 2 and 3 illustrate neurons from the CA1 and DG regions of P7 pups at 24–48 h after HI. Neurons from the contralateral hemisphere of P7 pups exhibited normal nuclear morphology and contained a normal distribution of polyribosomes, rough endoplasmic reticulum and mitochondria. In contrast, neurons from the ipsilateral CA1 (Fig. 2) and DG (Fig. 3) were severely damaged after HI. Three types of HI-injured neurons in P7 pups were observed by EM: (1) mixed features of apoptosis and necrosis (a chimera type; Fig. 2, 48 h, large arrows); (2) classical apoptosis with typical apoptotic features (Fig. 3, 48 h, white arrows); and (3), occasionally, cell lysis with normal nucleus and ruptured cell membrane (Fig. 4). The chimeric type of cell death was seen in most HI-injured CA1 neurons (Fig. 2, 48 h, arrows) and in a portion of HI-injured DG neurons (Fig. 3, black arrows). In this type of cell death, the cytoplasm and nucleus were shrunken, subcellular organelles were highly vacuolated although some mitochondria were still recognizable in the cytoplasm (Fig. 2, small arrows), and chromatin was partially clumped into irregularly shaped multi-chromatin masses (Fig. 2, large arrows). Formation of irregular-shaped multi-DNA masses in the nuclei appeared at approximately 24 h (Fig. 2, middle panel) and was still present at 48 h after HI (Fig. 2, right panel, arrows). The irregular multi-chromatin masses in HI-damaged neurons could be easily distinguished from the larger single chromatin balls typical for apoptotic neurons (Fig. 3, 48 h, middle panel, white arrows). Classical apoptotic features originally described by Kerr et al.(1972) were clearly visible in a portion of P7 DG neurons after HI (Fig. 3). These apoptotic features include clumping of chromatin into larger chromatin ball(s) that were displaced to one pole of the cell (Fig. 3, middle panel, white arrows), shrinkage of the entire cell, formation of filament bundles with membrane blebbing (Fig. 3, middle panel, black arrowheads), and phagocytes attaching to the apoptotic neurons (Fig. 3, middle panel, white arrowheads). These HI-injured DG neurons with apoptotic features were virtually comparable with developing neurons undergoing apoptosis under physiological conditions (Ishimaru et al., 1999). Some HI-injured DG neurons contained both irregular-shaped multi-chromatin masses as well as regular chromatin balls (Fig. 3, right panel, arrows). Some HI-injured DG neurons possesseda small chromatin ball with irregular edge (Fig. 3, right panel, black arrowheads), which have been previously posited to represent an early stage of formation of larger chromatin ball during apoptosis (Ishimaru et al., 1999). Occasionally, conventional necrotic neurons (cell lysis) with normal nuclear size but without cell membranes (ruptured) were observed in HI-injured brain regions (Fig. 4). Morphology of CA1 nucleus after membrane rupture appeared to be more irregular and more darkly stained under EM compared with control nucleus, likely due to changes in cell environment after membrane rupture (Fig. 4).

Changes in cell morphology were compared among HI-injured CA1 neurons at different ages (Fig. 5). As described above, most HI-injured CA1 neurons in P7 pups possessed small and irregular-shaped multi-chromatin masses in their nuclei (Fig. 5, P7, arrowheads), and recognizable mitochondria in the cytoplasm (Fig. 5, P7, arrows). With increasing age, the chromatin masses in CA1 neurons were reduced in size while the content of dispersed chromatin was correspondingly increased (Fig. 5, P15 and P26). By P60, nuclear chromatin in HI-injured CA1 neurons was mostly dispersed, while the nuclei exhibited a polygonal shape (Fig. 5, P60, arrows, also see Fig. 1C). These morphological features were mostly comparable to the shrinkage type of necrosis described previously after transient cerebral ischemia (Kirino and Sano, 1984; Deshpande et al., 1992; Colbourne et al., 1999; Ishimaru et al., 1999).

EM and confocal morphological features in HI-injured neurons

Ultrastructural features of HI-injured P7 neurons observed by EM were consistent with the nuclear morphology re-vealed by PI staining observed by confocal microscopy (Fig. 6). The multi-chromatin masses described as necrotic nuclei under EM (Fig. 6, EM panel, CA1, arrows) were similar in distribution and shape to those stained with PI (red) under confocal microscopy (Fig. 6, PI panel, CA1, arrows). These PI-stained multi-DNA masses looked larger under confocal microscopy than the chromatin masses under EM (Fig. 6, CA1, EM). This discrepancy was likely because the tissue sections for confocal microscopy (50 μm) were much thicker than the ultrathin sections for EM (0.1 μm). The larger regular chromatin ball typical for apoptosis under EM in P7 pups after HI (Fig. 6, EM panel, DG, arrows) appeared to correspond to the densely stained nuclear ball under confocal microscopy (Fig. 6, PI panel, DG, large arrows). Neurons with either the irregular multi-DNA masses or the larger regular DNA balls were strongly positive for active caspase-3 (Fig. 6, PI+Cas, green), indicating that caspase-3-mediated biochemical processes were highly active in both types of HI-injured neurons.

Time course of cell death after HI in developing neurons

To study the time course of neuronal death after HI in developing rats, P15 rats were subjected to HI followed by 6, 24 and 48 h of recovery (Fig. 7). Brain sections were double-labeled with active caspase-3 and PI, and examined by confocal microscopy. As illustrated in Fig. 7, HI-injured neurons, as judged by their shrunken and fragmented nuclei stained with PI under confocal microscopy (see Fig. 1C), appeared as early as 6 h, and significantly increased in number further from 24 h–48 h after HI in the DG (Fig. 7, left panel). In comparison, HI-injured neurons were rarely found in CA1 until 24 h–48 h after HI (Fig. 7, left panel). Both cell bodies and small dendritic trees of HI-injured DG neurons were clearly labeled with activecaspase-3 at 6 h after HI (Fig. 7, right panel), whereas mainly cell bodies and dendritic trunks were stained with active caspase-3 at 48 h after HI (see Fig. 6), suggesting that small dendritic trees might already be degenerated at 48 h in these neurons after HI.

Quantitative study of active caspase-3 positive and negative neurons

To study quantitatively the changes in active caspase-3 positive and negative neurons after HI as a function of developing age, we counted the total number of dead neurons, as well as the total number of active caspase-3 positive and negative neurons in the ipsilateral CA1 and DG regions at the level of Bregma −4.0 mm (see Fig. 1A and Table 1). We also counted the number of normal neurons in the CA1 and DG regions of the contralateral hemisphere (Table 1). The total number of neurons in the contralateral hippocampus significantly declined with increasing age, consistent with normal brain development (Bayer and Altman, 1995). After HI, the number of active caspase-3 positive neurons declined. In the CA1 region, the average number of active caspase-3 positive neurons per field was reduced from 109.69±6.92% in P7 pups, to 32.77±9.40% in P15 pups, to 0.88±0.90% in P26 rats, and to 0.27±0.47% in P60 rats, respectively (Table 1). In the DG area, a similar decline in the number of active caspase-3 positive neurons was observed with increasing age (Table 1). However, in P26 rats after HI, the number of active caspase-3 positive neurons was significantly higher in the DG area (14.13±8.20%) relative to that in the CA1 region (0.88±0.90%), coincident with the fact that DG neurons are continuously developing through adulthood (Bayer and Altman, 1995).

DISCUSSION

In the present study, we investigated the pathogenesis of HI-induced neuronal death in rats at different postnatal ages. After a period of HI, most neurons in the ischemic region

underwent delayed neuronal death at all ages. However, the results from the present study suggest that the mechanisms underlying delayed neuronal death alter as a function of brain development. In P7 pups, despite more than 95% of HI-injured neurons highly expressing active caspase-3, most of these active caspase-3 positive neurons revealed mixed features of apoptosis and necrosis (a chimera type) under EM. Classical apoptosis was observed only in small populations of HI-injured P7 neurons. Furthermore, in rats older than P7, most HI-injured neurons displayed features of necrotic cell death under EM and, concomitantly, active caspase-3 positive neurons after HI declined dramatically. In P60 rats, virtually all HI-injured neurons showed the shrinkage necrotic morphology under EM and were negative for active caspase-3. These results strongly suggest that pathogenesis of HI-induced neuronal death is shifting from apoptosis to necrosis during brain development.

Ultrastructural analysis revealed that only small populations of HI-injured neurons exhibited classic features of apoptosis, although HI-injured neurons at earlier developmental ages are highly positive for active caspase-3. For example, most CA1 neurons after HI were positive for active caspase-3 at age 7 days, but they did not exhibit classic features of apoptosis under EM, rather they more closely resembled the shrinkage type of necrosis described in many previous EM studies (Kirino and Sano, 1984; Smith et al., 1988; Yamamoto et al., 1990; Deshpande et al., 1992; Ishimaru et al., 1999; Fukuda et al., 1999; Colbourne et al., 1999; Hu et al., 2000b). In the DG region, only a portion of neurons, mostly in the inner layer of DG, displayed classic features of apoptosis, whereas the rest of the DG neurons exhibited either mixed features of apoptosis and necrosis, or the shrinkage type of necrosis at age P7 after HI (see Figs. 2–3). These results suggest that both apoptotic and necrotic mechanisms of cell death remain significant in developing neurons after HI.

Both neuronal apoptosis and necrosis have repeatedly been observed in neonatal HI models (Mehmet et al., 1994; Portera-Cailliau et al., 1997; Martin et al., 1998; Pulera et al., 1998; Renolleau et al., 1998; Ishimaru et al., 1999; Nakajima et al., 2000; Sheldon et al., 2001), whereas apoptosis has inconsistently been reported in adult neurons after hypoxia or ischemia (Deshpande et al., 1992; Fukuda et al., 1999; Colbourne et al., 1999). One source of confusion may be the methodology used for cell classification. Apoptosis and necrosis have distinct morphology, and EM is necessary to distinguish between them (Kerr et al., 1972; Ishimaru et al., 1999). EM was originally utilized to characterize cell apoptosis and still remains the indisputable tool for identifying apoptotic cells (Ishimaru et al., 1999; Sheldon et al., 2001; Watanabe et al., 2002). Other methods for apoptosis are relatively non-specific. Analyses of DNA fragmentation have been very widely used, but it has been repeatedly reported that this type of analysis is incapable of distinguishing apoptosis from necrosis (Enright et al., 1994; van Lookeren Campagne et al., 1995; Grasl-Kraupp et al., 1995; Charriaut-Marlangue and Ben-Ari, 1995; de Torres et al., 1997; Ishimaru et al., 1999; Zhu et al., 2000). Ishimaru et al. (1999) pointed out that ultrastructural analysis provided an unambiguous means of distinguishing between excitotoxic and apoptotic neurodegeneration after brain injury, whereas DNA fragmentation analysis (TUNEL staining or gel electrophoresis) was of no value because these tests were positive for both apoptosis and necrosis. Biochemical makers of apoptosis have also been widely used to study biochemical cascades of apoptosis after injury, but, as demonstrated in the present study, most HI-injured developing neurons with morphological features of necrosis are still highly positive for active caspase-3, a biochemical marker of apoptosis. Other biochemical markers, such as translocation of cytochrome c from mitochondria to cytoplasm or activation of proapoptotic proteins such as Bax, may indicate or cause mitochondrial damage after brain ischemia. Therefore, they may not be reliable biochemical markers exclusively for apoptosis.

Although some of the conflicting results regarding the nature of cell death after HI may be due to methodological issues, some may also result from animal developmental stage or the

time points after injury at which ischemic cell death is investigated. Based on EM studies of the type of cell death in P7 pups after HI, Martin et al. (1998) proposed that cell death proceeds along a continuum from apoptosis (early injury) to necrosis (late injury). Ishimaru et al. (1999) found that transient HI-induced neuronal death in neonates was mostly identical to glutamate-induced neurodegeneration in the hypothalamus, but was fundamentally different from classical apoptosis. Sheldon et al. (2001) suggested that the cell death was neither apoptotic nor necrotic, but rather a novel type of cell death. In adult mouse brains after transient HI, neither classical apoptosis nor the cell rupture type of necrosis was observed (Fukuda et al., 1999). Indeed, numerous studies demonstrate that neurons undergoing delayed neuronal death after injury rarely exhibit cell swelling followed by rupture, i.e. conventional necrosis, but rather they exhibit a shrinkage type of necrosis, similar to the necrosis described after transient cerebral ischemia (Kirino and Sano, 1984; Smith et al., 1988; Deshpande et al., 1992; van Lookeren-Campagne and Gill, 1996; Petito et al., 1997; Colbourne et al., 1999). The present study demonstrates that most HI-injured developing neurons in P7 pups displayed mixed features of apoptosis and necrosis under EM but they were highly positive for active caspase-3, a key player in apoptotic biochemical cascades. Therefore, delayed neuronal death in most developing neurons after HI is a mixture of apoptosis and necrosis. This coexistence of apoptosis and necrosis shifts toward necrosis during brain development, and neurons in adult brain probably will die mostly by necrosis after injury due to the lack of expression of apoptotic genes. However, this study by no means excludes the possibility that brain cells other than postmitotic neurons, such as endothelial cells and glial cells, particularly the newly proliferated ones, may die by apoptosis after ischemia.

This study provides additional evidence that the pathogenesis of cell death due to HI changes during brain development. This novel information is consistent with the concept that the mechanism of cell death after brain ischemia is quite different between developing and adult brains (Clarke, 1990; Johnston et al., 1995; Johnston et al., 2002). While it may seem only an academic exercise to debate whether delayed neuronal death after injury is apoptotic, it is worthwhile to understand the molecular events underlying HI-induced cell death in neurons at different developmental ages, and to investigate whether an antiapoptotic strategy should be considered for treatment of brain injury at different ages. Although the true classic features of apoptosis under EM were only found in small populations of immature neurons in P7 pups after HI, biochemical events of apoptosis such as activation of caspase-3 are actively taking place in most developingneurons after HI (Puka-Sundvall et al., 2000; Nakajima et al., 2000; Han et al., 2000; Wang et al., 2001; Northington et al., 2001; Zhu et al., 2003). It is, therefore, likely that immature neurons are liable to apoptosis after injury (Ikonomidou et al., 1989; Johnston, 1995), and thus both necrosis and apoptosis remain effective therapeutic targets for developing neurons after brain injury (Han et al., 2000; Cheng et al., 1998; Nakajima et al., 2000; Northington et al., 2001; Blomgren et al., 2001). However, both apoptotic morphology and biochemical machinery fade out during brain development. Therefore, traditional approaches targeting to necrotic cell death mechanisms such as energy failure, acidosis, calcium influx, oxidative stress and protein aggregation in adult brain remain valid.

Acknowledgments

This work was supported by National Institutes of Health grants NS40407 (B.R.H.).

Abbreviations

CCA common carotid artery

DG	dentate gyrus
EM	electron microscopy
HI	hypoxia-ischemia
P	postnatal day
PBS	phosphate-buffered saline
PI	propidium iodide
TX100	Triton X-100

REFERENCES

Auer RN, Olsson Y, Siesjö BK. Hypoglycemic brain injury in the rat: correlation of density of brain damage with the EEG isoelectric time: a quantitative study. Diabetes. 1984; 33:1090–1098. [PubMed: 6500189]

Bayer, SA.; Altman, J. Neurogenesis and neuronal migration. In: Paxinos, G., editor. The rat nervous system. 1995. p. 1044-1078.

Blomgren K, Zhu C, Hallin U, Hagberg H. Mitochondria and ischemic reperfusion damage in the adult and in the developing brain. Biochem Biophys Res Commun. 2003; 304:551–559. [PubMed: 12729590]

Blomgren K, Zhu C, Wang X, Karlsson JO, Leverin AL, Bahr BA, Mallard C, Hagberg H. Synergistic activation of caspase-3 by *m*-calpain after neonatal hypoxia-ischemia: a mechanism of "pathological apoptosis"? J Biol Chem. 2001; 276:10191–10198. [PubMed: 11124942]

Blumenfeld KS, Welsh FA, Harris VA, Pesenson MA. Regional expression of c-fos and heat shock protein-70 mRNA following hypoxia-ischemia in immature rat brain. J Cereb Blood Flow Metab. 1992; 12:987–995. [PubMed: 1400653]

Charriaut-Marlangue C, Ben-Ari Y. A cautionary note on the use of the TUNEL stain to determine apoptosis. Neuroreport. 1995; 7:61–64. [PubMed: 8742417]

Cheng Y, Deshmukh M, D'Costa A, Demaro JA, Gidday JM, Shah A, Sun Y, Jacquin MF, Johnson EM, Holtzman DM. Caspase inhibitor affords neuroprotection with delayed administration in a rat model of neonatal hypoxic-ischemic brain injury. J Clin Invest. 1998; 101:1992–1999. [PubMed: 9576764]

Clarke PG. Developmental cell death: morphological diversity and multiple mechanisms. Anat Embryol (Berl). 1990; 181:195–213. [PubMed: 2186664]

Colbourne F, Sutherland GR, Auer RN. Electron microscopic evidence against apoptosis as the mechanism of neuronal death in global ischemia. J Neurosci. 1999; 19:4200–4210. [PubMed: 10341224]

de Torres C, Munell F, Ferrer I, Reventós J, Macaya A. Identification of necrotic cell death by the TUNEL assay in the hypoxicischemic neonatal rat brain. Neurosci Lett. 1997; 230:1–4. [PubMed: 9259449]

Deshpande J, Bergstedt K, Linden T, Kalimo H, Wieloch T. Ultrastructural changes in the hippocampal CA1 region following transient cerebral ischemia: evidence against programmed cell death. Exp Brain Res. 1992; 88:91–105. [PubMed: 1371756]

Dodson RF, Aoyagi M, Hartmann A, Tagashira Y. Acute cerebral infarction and hypotension: an ultrastructural study. J Neuropathol Exp Neurol. 1974; 33:400–407. [PubMed: 4365913]

Enright H, Hebbel RP, Nath KA. Internucleosomal cleavage of DNA as the sole criterion for apoptosis may be artifactual. J Lab Clin Med. 1994; 124:63–68. [PubMed: 8035105]

Fukuda T, Wang H, Nakanishi H, Yamamoto K, Kosaka T. Novel non-apoptotic morphological changes in neurons of the mouse hippocampus following transient hypoxic-ischemia. Neurosci Res. 1999; 33:49–55. [PubMed: 10096471]

Gill R, Soriano M, Blomgren K, Hagberg H, Wybrecht R, Miss MT, Hoefer S, Adam G, Niederhauser O, Kemp JA, Loetscher H. Role of caspase-3 activation in cerebral ischemia-induced

neurodegeneration in adult and neonatal brain. J Cereb Blood Flow Metab. 2002; 22:420–430. [PubMed: 11919513]

Grasl-Kraupp B, Ruttkay-Nedecky B, Koudelka H, Bukowska K, Bursch W, Schulte-Hermann R. In situ detection of fragmented DNA (TUNEL assay) fails to discriminate among apoptosis, necrosis, and autolytic cell death: a cautionary note. Hepatology. 1995; 21:1465–1468. [PubMed: 7737654]

Han BH, D'Costa A, Back SA, Parsadanian M, Patel S, Shah AR, Gidday JM, Srinivasan A, Deshmukh M, Holtzman DM. BDNF blocks caspase-3 activation in neonatal hypoxia-ischemia. Neurobiol Dis. 2000; 7:38–53. [PubMed: 10671321]

Hu BR, Liu CL, Ouyang Y, Blomgren K, Siesjö BK. Involvement of caspase-3 in cell death after hypoxia-ischemia declines during brain maturation. J Cereb Blood Flow Metab. 2000a; 20:1294–1300. [PubMed: 10994850]

Hu BR, Martone ME, Jones YZ, Liu CL. Protein aggregation after transient cerebral ischemia. J Neurosci. 2000b; 20:3191–3199. [PubMed: 10777783]

Ikonomidou C, Mosinger JL, Salles KS, Labruyere J, Olney JW. Sensitivity of the developing rat brain to hypobaric/ischemic damage parallels sensitivity to *N*-methyl-aspartate neurotoxicity. J Neurosci. 1989; 9:2809–2818. [PubMed: 2671294]

Ishimaru MJ, Ikonomidou C, Tenkova TI, Der TC, Dikranian K, Sesma MA, Olney JW. Distinguishing excitotoxic from apoptotic neurodegeneration in the developing rat brain. J Comp Neurol. 1999; 408:461–476. [PubMed: 10340498]

Johnston MV. Neurotransmitters and vulnerability of the developing brain. Brain Dev. 1995; 17:301–306. [PubMed: 8579213]

Johnston MV, Nakajima W, Hagberg H. Mechanisms of hypoxic neurodegeneration in the developing brain. Neuroscientist. 2002; 8:212–220. [PubMed: 12061501]

Kerr JF, Wyllie AH, Currie AR. Apoptosis: a basic biological phenomenon with wide-ranging implications in tissue kinetics. Br J Cancer. 1972; 26:239–257. [PubMed: 4561027]

Kirino T, Sano K. Fine structural nature of delayed neuronal death following ischemia in the gerbil hippocampus. Acta Neuropathol (Berl). 1984; 62:209–218. [PubMed: 6695555]

Martin LJ, Al-Abdulla NA, Brambrink AM, Kirsch JR, Sieber FE, Portera-Cailliau C. Neurodegeneration in excitotoxicity, global cerebral ischemia, and target deprivation: a perspective on the contributions of apoptosis and necrosis. Brain Res Bull. 1998; 46:281–309. [PubMed: 9671259]

Mehmet H, Yue X, Squier MV, Lorek A, Cady E, Penrice J, Sarraf C, Wylezinska M, Kirkbride V, Cooper C, et al. Increased apoptosis in the cingulate sulcus of newborn piglets following transient hypoxia-ischaemia is related to the degree of high energy phosphate depletion during the insult. Neurosci Lett. 1994; 181:121–125. [PubMed: 7898750]

Nakajima W, Ishida A, Lange MS, Gabrielson KL, Wilson MA, Martin LJ, Blue ME, Johnston MV. Apoptosis has a prolonged role in the neurodegeneration after hypoxic ischemia in the newborn rat. J Neurosci. 2000; 20:7994–8004. [PubMed: 11050120]

Northington FJ, Ferriero DM, Flock DL, Martin LJ. Delayed neurodegeneration in neonatal rat thalamus after hypoxia-ischemia is apoptosis. J Neurosci. 2001; 21:1931–1938. [PubMed: 11245678]

Olney JW. Excitotoxicity, apoptosis and neuropsychiatric disorders. Curr Opin Pharmacol. 2003; 3:101–109. [PubMed: 12550750]

Petito CK, Torres-Munoz J, Roberts B, Olarte JP, Nowak TSJ, Pulsinelli WA. DNA fragmentation follows delayed neuronal death in CA1 neurons exposed to transient global ischemia in the rat. J Cereb Blood Flow Metab. 1997; 17:967–976. [PubMed: 9307610]

Portera-Cailliau, Price DL, Martin LJ. Excitotoxic neuronal death in the immature brain is an apoptosis-necrosis morphological continuum. J Comp Neurol. 1997; 378:70–87. [PubMed: 9120055]

Puka-Sundvall M, Wallin C, Gilland E, Hallin U, Wang X, Sandberg M, Karlsson J, Blomgren K, Hagberg H. Impairment of mitochondrial respiration after cerebral hypoxia-ischemia in immature rats: relationship to activation of caspase-3 and neuronal injury. Brain Res Dev Brain Res. 2000; 125:43–50.

Pulera MR, Adams LM, Liu H, Santos DG, Nishimura RN, Yang F, Cole GM, Wasterlain CG. Apoptosis in a neonatal rat model of cerebral hypoxia-ischemia. Stroke. 1998; 29:2622–2630. [PubMed: 9836776]

Renolleau S, Aggoun-Zouaoui D, Ben-Ari Y, Charriaut-Marlangue C. A model of transient unilateral focal ischemia with reperfusion in the P7 neonatal rat: morphological changes indicative of apoptosis. Stroke. 1998; 29:1454–1460. [PubMed: 9660403]

Sheldon RA, Hall JJ, Noble LJ, Ferriero DM. Delayed cell death in neonatal mouse hippocampus from hypoxia-ischemia is neither apoptotic nor necrotic. Neurosci Lett. 2001; 304:165–168. [PubMed: 11343828]

Siesjö BK. Oxygen deficiency and brain damage: localization, evolution in time, and mechanisms of damage. J Toxicol Clin Toxicol. 1985; 23:267–280. [PubMed: 4057318]

Smith ML, Kalimo H, Warner DS, Siesjö BK. Morphological lesions in the brain preceding the development of postischemic seizures. Acta Neuropathol (Berl). 1988; 76:253–264. [PubMed: 3213428]

Towfighi J, Mauger D. Temporal evolution of neuronal changes in cerebral hypoxia-ischemia in developing rats: a quantitative light microscopic study. Brain Res Dev Brain Res. 1998; 109:169–177.

Towfighi J, Mauger D, Vannucci RC, Vannucci SJ. Influence of age on the cerebral lesions in an immature rat model of cerebral hypoxia-ischemia: a light microscopic study. Brain Res Dev Brain Res. 1997; 100:149–160.

van Lookeren, Campagne M.; Gill, R. Ultrastructural morphological changes are not characteristic of apoptotic cell death following focal cerebral ischaemia in the rat. Neurosci Lett. 1996; 213:111–114. [PubMed: 8858621]

van Lookeren, Campagne M.; Lucassen, PJ.; Vermeulen, JP.; Balázs, R. NMDA and kainate induce internucleosomal DNA cleavage associated with both apoptotic and necrotic cell death in the neonatal rat brain. Eur J Neurosci. 1995; 7:1627–1640. [PubMed: 7551189]

Wang X, Karlsson JO, Zhu C, Bahr BA, Hagberg H, Blomgren K. Caspase-3 activation after neonatal rat cerebral hypoxia-ischemia. Biol Neonate. 2001; 79:172–179. [PubMed: 11275647]

Watanabe M, Hitomi M, van der Wee K, Rothenberg F, Fisher SA, Zucker R, Svoboda KK, Goldsmith EC, Heiskanen KM, Nieminen AL. The pros and cons of apoptosis assays for use in the study of cells, tissues, and organs. Microsc Microanal. 2002; 8:375–391. [PubMed: 12533214]

Wyllie AH. Apoptosis: an overview. Br Med Bull. 1997; 53:451–465. [PubMed: 9374030]

Yamamoto K, Hayakawa T, Mogami H, Akai F, Yanagihara T. Ultrastructural investigation of the CA1 region of the hippocampus after transient cerebral ischemia in gerbils. Acta Neuropathol (Berl). 1990; 80:487–492. [PubMed: 2251905]

Zhu C, Qiu L, Wang X, Hallin U, Cande C, Kroemer G, Hagberg H, Blomgren K. Involvement of apoptosis-inducing factor in neuronal death after hypoxia-ischemia in the neonatal rat brain. J Neurochem. 2003; 86:306–317. [PubMed: 12871572]

Zhu C, Wang X, Hagberg H, Blomgren K. Correlation between caspase-3 activation and three different markers of DNA damage in neonatal cerebral hypoxia-ischemia. J Neurochem. 2000; 75:819–829. [PubMed: 10899960]

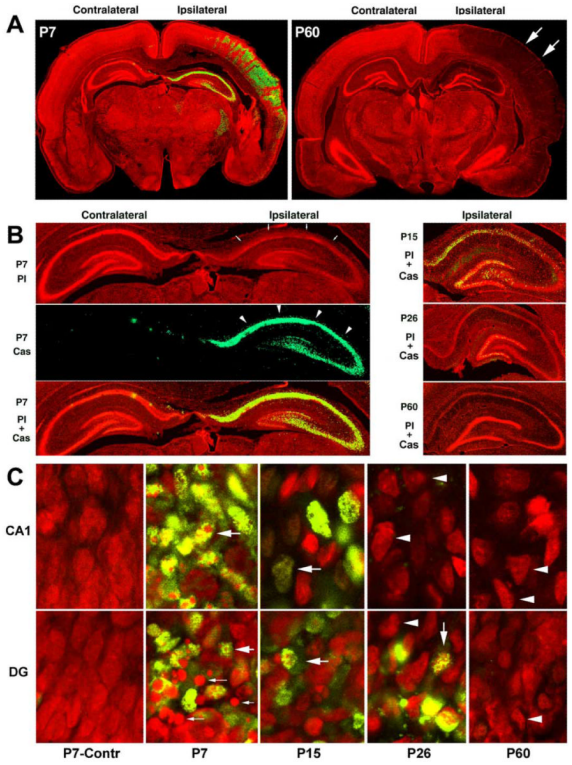

Fig. 1.

(A) Montages of confocal images from brain sections double-stained with anti-active caspase-3 (green) and PI (red). P7 pups and P60 rats were subjected to HI followed by 48 h of recovery. Nucleic acids in the brain sections were stained with PI in red, while active caspase-3 was stained in green. HI-injured regions were recognizable by the weaker PI staining (arrows), and they were highly positive for active caspase-3 (green) in P7 pups, but negative in P60 rats. (B) High magnification of the hippocampal regions. The sections from P7, P15, P26 and P60 rats were subjected to HI followed by 48 h of recovery. The PI staining was dim in the HI-injured areas (P7-PI, red panel, arrows in B). Active caspase-3 immunolabeling was the strongest in the ipsilateral hippocampal regions of P7 pups (P7 Cas, the green panel, arrows), but declined markedly at P15 and P26, and was virtually absent in P60 rats. (C) Higher magnification of the confocal images from the hippocampal CA1 and DG regions. Most HI-injured P7 CA1 and DG neurons were positive for active caspase-3 (green). The PI-stained multi-DNA masses were mostly seen in the CA1 and in a portion of DG neurons of P7 pups after HI (red, large arrows). The large DNA balls were seen in another portion of HI-injured DG neurons of P7 pups (P7, DG, small arrows). Both active caspase-3 positive neurons and sizes of multi-DNA masses after HI decreased progressively in P15 and P26 rats. In most HI-injured neurons of P60 rats, active caspase-3 was virtually negative and the chromatin masses became smaller or dispersed (arrowheads).

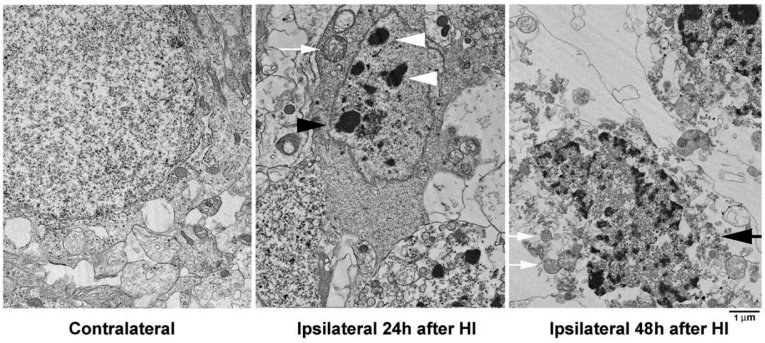

Fig. 2.

Electron micrographs of P7 CA1 neurons from the contralateral and ipsilateral hemispheres at 24 and 48 h after HI. Ultrastructure of the contralateral neurons was normal. HI-injured CA1 neurons started to form irregular-shaped multi-chromatin masses at 24 h (middle panel, arrowhead) and were further shrunken at 48 h after HI (large arrow); subcellular organelles were vacuolated; but some mitochondria were still recognizable (small arrows).

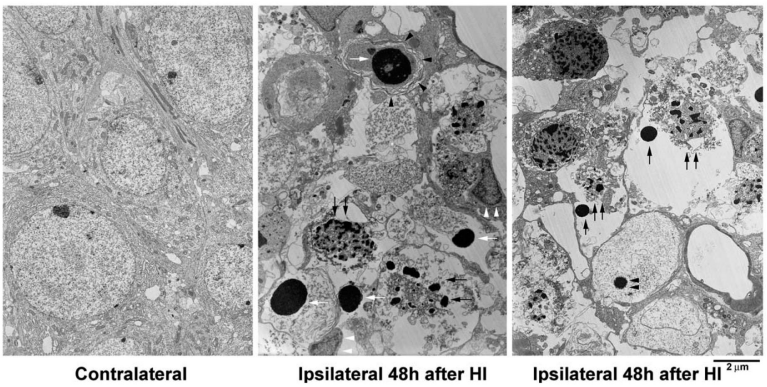

Fig. 3.

Electron micrographs of P7 DG neurons from the contralateral and ipsilateral hemispheres at 48 h after HI. Ultrastructure of the contralateral neurons was normal, while the ipsilateral neurons were severely damaged after HI. Two types of nuclei were observed in HI-injured DG granule cells: small and irregular-shaped multi-chromatin masses (middle panel, black arrows), and large and regular-shaped chromatin balls (middle panel, white arrows). The membrane became filament bundles (middle panel, black arrowheads) and phagocytes attached to the apoptotic neurons (middle panel, white arrowheads). Both the irregular-shaped multi-chromatin masses and the regular-shaped chromatin balls were found in the same DG nuclei (right panel, arrows). A small chromatin ball with irregular edge was seen in an HI-injured DG neuron (right panel, arrowheads).

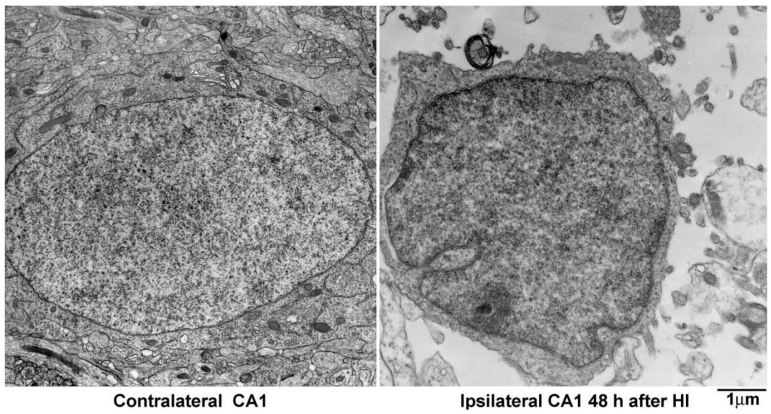

Fig. 4.

Electron micrographs of P7 CA1 neurons from the contralateral and ipsilateral hemispheres at 48 h after HI. The contralateral neuron was normal, while the ipsilateral neuron was necrotic with nucleus but without intact cell membrane. The contents of the cytoplasm were released.

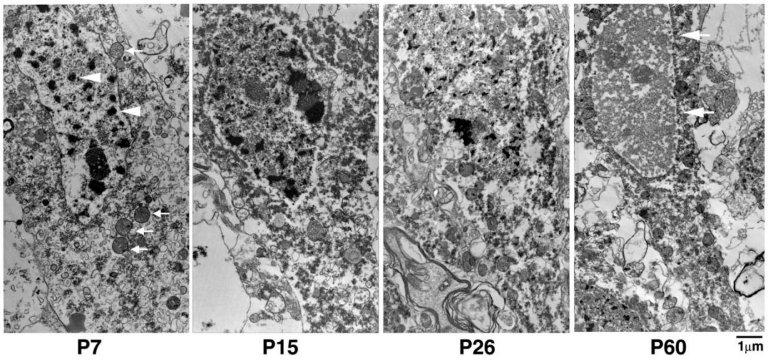

Fig. 5.

Electron micrographs of CA1 neurons at different ages. The EM sections were from the ipsilateral CA1 pyramidal layer of P7, P15 P26 and P60 rats subjected to HI followed by 48 h of recovery. In P7 pups, the nucleus exhibited irregular-shaped multi-chromatin masses (arrowheads), and several mitochondria were still intact (arrows). In P15 and P26 rats, the multi-chromatin masses tended to decrease in size. In P60 rats, the nuclear chromatin was mostly dispersed and the nucleus was polygonal shaped (arrows).

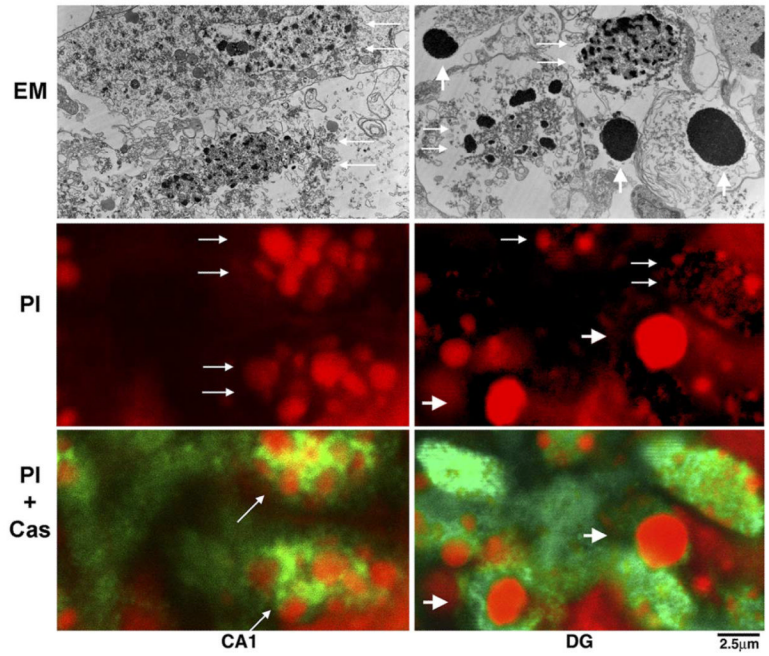

Fig. 6.

Comparison of EM features with features under confocal microscopy in HI-injured CA1 and DG neurons of P7 pups. The multi-chromatin masses seen in CA1 and DG nuclei under EM (EM panel, small arrows) were highly stained with PI under confocal microscopy (PI panel, small arrows). The large DNA balls under EM in the HI-injured DG area (EM panel, large arrows) were also highly stained with PI (PI panel, large arrows). Both HI-injured CA1 and DG neurons with either the multi-DNA masses or the large DNA balls were highly positive for active caspase-3 (PI+Cas panel, arrows).

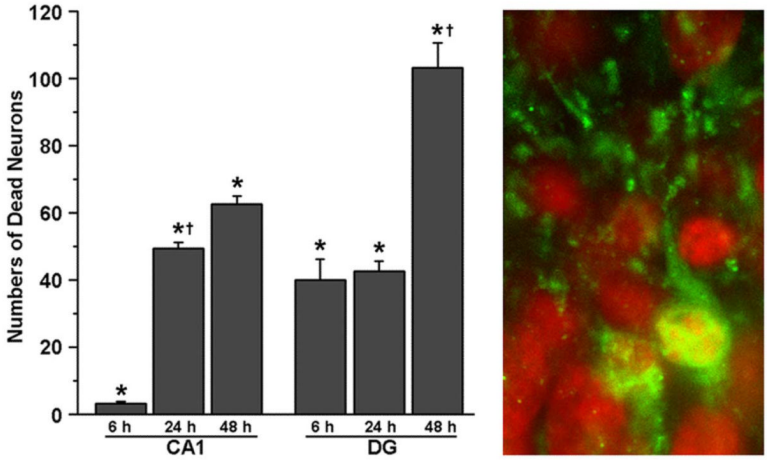

Fig. 7.

Time course of neuronal death after HI. Brain sections were from P15 rats subjected to HI followed by 6, 24 and 48 h of recovery. They were double-labeled with active caspase-3 (green) and PI (red) and examined by confocal microscopy. Average numbers of dead cells were counted in a field of 175 μm×175 μm (60× objective field) on the brain sections at 6, 24 and 48 h after HI. The data are expressed as mean±S.D. from four rats in each group. * Indicates significant differences between sham-operative control and 6, 24 or 48 h in the CA1 and DG regions ($P<0.01$, Fisher's PLSD test). † Denotes significant difference between 6 h and 24 h after HI in CA1 region, and between 24 h and 48 h after HI in DG area ($P<0.01$, Fisher's PLSD test). The right panel shows confocal images of HI-injured P15 DG region at 6 h after HI. The active caspase-3 (green) was distributed not only in cell bodies but also in the dendritic trees.

Table 1

Average numbers of active caspase-3 positive/negative and total normal and dead neurons after HI in hippocampal regions at different developmental stages[a]

Groups	Total normal neurons	Total dead neurons	Positive cells	Negative cells
CA1 region				
P7	129.63±17.60	115.23±7.47	109.69±6.92	5.54±3.53
P15	64.64±13.89*	62.81±11.46*	32.77±9.40*	30.03±8.38*
P26	59.57±5.13*	61.29±18.46*	0.88±0.90*	60.43±18.18*
P60	50.27±3.23*	46.36±8.79*	0.27±0.47*	46.09±8.68
DG area				
P7	163.17±28.67	112.67±18.78	108.00±19.51	4.68±2.42
P15	155.67±24.32	106.33±42.69	56.17±25.90*	50.17±19.24*
P26	123.88±17.61*	66.63±5.61*	14.13±8.20*	52.50±9.68*
P60	102.22±13.69*	73.91±23.45*	1.82±1.66*	72.10±23.98*

[a]The numbers of total normal neurons were counted in the contralateral hippocampal sections, whereas the numbers of active caspase 3 positive/negative as well as total dead neurons were counted in the ipsilateral hippocampal sections in a field of 175 μm×175 μm (60× objective field of confocal microscopy; see the Experimental Procedures section). The data are expressed as mean±S.D. from four rats in each group.

*$P<0.01$ denotes significant difference between the P7 group and other age groups (Fisher's PLSD test).